Iran Polym J (2015) 24:697–704
DOI 10.1007/s13726-015-0361-0

ORIGINAL PAPER

Water-repellent flexible fabric strain sensor based on polyaniline/titanium dioxide-coated knit polyester fabric

Xiaoning Tang[1,2] · Mingwei Tian[1,2,3] · Lijun Qu[1,2,3] · Shifeng Zhu[1,2] · Xiaoqing Guo[1,2,3] · Guangting Han[2,3] · Kaikai Sun[1,2]

Received: 29 January 2015 / Accepted: 29 June 2015 / Published online: 11 July 2015

Abstract A flexible fabric strain sensor was prepared by in situ chemical polymerization of aniline on knit polyester fabric surface in aqueous acid solutions using ammonium persulfate as an oxidant. Furthermore, the optimum addition ratio of titanium dioxide (TiO_2) in polyaniline (PANI) in the granular conductive network membrane was investigated. The morphological, structural, thermal, electrical, strain-sensing, and water-repellent properties of the polyester knit fabrics modified with PANI and PANI/TiO_2 hybrid were analyzed. The surface electrical resistance of PANI/TiO_2 conductive films on the knit fabric was higher than that of pristine PANI, which was due to the particle blocking the conduction path effect caused by TiO_2 embedded in the PANI matrix. However, it was further found that the addition of TiO_2 could improve the durability properties of flexible fabric strain sensor against cycles of elongation, though with a little loss in electrical conductivity and sensitivity. Moreover, the water-repellent property was evaluated by measuring water contact angles. The results showed that for PANI/TiO_2 nanocomposites-coated flexible fabric strain sensor, a desirable level of contact angle (127.5° ± 1.7°) was even preserved at 121.8° ± 2.6° after 100 cycles of elongation. This indicated that the flexible fabric strain sensor had rather high water-repellent efficiency and excellent durability during the elongation cycles.

Keywords Polyaniline · Titanium dioxide · Flexible fabric strain sensor · Electrical conductivity · Water repellent

Introduction

Intelligent textile materials can sense and react to environmental conditions and respond to or be activated to perform a function by manual operation or in a pre-programmed manner, which can be used for the preparation of wearable devices for training, fitting, rehabilitation, etc. [1]. An important step in this direction involves the development of flexible strain-sensing fabric for the detection of strain to enable the measurement and control of various movements of the human body. For instance, Farringdon et al. [2] built a knit strain sensor which was integrated into a jacket and used to measure human body movements. Rossi et al. [3, 4] developed a strain-sensing glove based on the fabrication of polypyrrole-coated Lycra/cotton sensing fabric. Despite several promising advances in the emerging research field of flexible strain sensor, a number of obstacles still exist. For instance, the relatively low sensitivity and durability and weak resistance against water; thus, it is urgent to develop flexible fabric strain sensors with excellent water-repellent efficiency and durability against repeated cycles of elongation. Consequently, great effort has been made in the present work to prepare flexible fabric strain sensor with sufficient electrical sensitivity, flexibility, water repellency, and durability as well as intelligent functionality.

X. Tang and M. Tian have contributed equally to this paper.

✉ Mingwei Tian
tmw0303@126.com

✉ Lijun Qu
profqu@126.com

[1] College of Textiles, Qingdao University, Qingdao 266071, Shandong, China

[2] Laboratory of New Fiber Materials and Modern Textile, the Growing Base for State Key Laboratory, Qingdao University, Qingdao 266071, Shandong, China

[3] Collaborative Innovation Center for Marine Biomass Fibers, Materials and Textiles of Shandong Province, Qingdao University, Qingdao 266071, Shandong, China

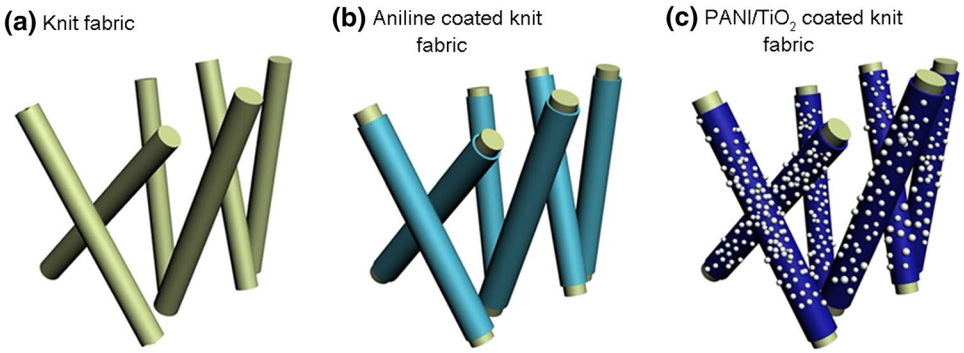

Fig. 1 Schematic diagram of hybrid-coated knit fabric preparation

Polyaniline (PANI) is one of the most promising conductive polymers because of its environmental stability, low cost, controllable electrical conductivity, and interesting redox properties [5–8]. However, PANI is susceptible to rapid degradation in properties upon repetitive cycles (charge/discharge process), because of its swelling and shrinkage. To alleviate this limitation, the combination of PANI with fine-grade filler materials, such as carbon nanotube [9], graphene [10, 11], mesoporous carbon [12], ZnO [13, 14], SiO_2 [15], NiO [16], and Fe_3O_4 [17], has already been reported. For instance, Kachoei et al. [18] prepared graphene/emeraldine salt composites with sandwich-like structures via in situ inverse microemulsion polymerization of aniline monomers. It was further found that the composites exhibited enhanced electrical properties and thermal stability, which helped to evoke a novel electrical conductive material for fabricating electrochemical devices. Organic and inorganic hybrid materials are gaining much importance and research attention due to their wide applications [19].

The existing and promising applications of TiO_2 nanomaterials include UV protection, photocatalysis, sensing, self-cleaning, and electrochromics as well as water repellence [20–23]. Furthermore, the properties of TiO_2-based nanocomposites can be varied by introducing various amounts of TiO_2. It is reported that TiO_2 may act as a suitable template for the formation of well-oriented polyaniline and electrical conductivity can be enhanced by developing better orientated defect-free conducting polymers [24, 25]. The excellent stability in electrical conductivity is given by virtue of electron donor–acceptor interactions between polyaniline and TiO_2 [26]. The increased amount of TiO_2 may hinder the carrier transport between different molecular chains of polyaniline and thus decrease the electrical conductivity of polyaniline–TiO_2 hybrids [27]. These hybrids have better processibility than the pristine inorganic component, as reported [28–30]. However, to the best of our knowledge, polyaniline–TiO_2 coatings performed on knit fabric to fabricate water-repellent flexible strain sensor have not been reported.

In this work, nano-TiO_2 was used as a filler to prepare PANI/TiO_2 composites coated on PET knit fabric by an in situ polymerization method. Also, the optimum addition amount of TiO_2 nanoparticles was investigated. Furthermore, the electrical conductivity, sensitivity, durability, and water-repellent properties of the flexible fabric strain sensor were investigated.

Experimental

Materials

Aniline (AN) was purchased from Tianjin Fine Chemical Research Institute, and fine-grade TiO_2 (about 25 nm in diameter) was supplied by Shanghai Yuejiang Titanium Chemical Manufacture Co., Ltd. All other reagents used in this study were of analytical grade and used as such without any further purification. Polyester knit fabric of 40s count was obtained from Qingdao Jifa Group Co., Ltd.

Preparation of hybrid-coated knit fabric

The fabric coatings were prepared by in situ polymerization process. In detail, 6 cm × 7 cm fabrics without crease were immersed in a bottle containing 10 mL aniline monomer and 40 mL anhydrous ethyl alcohol for 60 min. Then, required amounts of ammonium persulfate (APS) at 1:1 molar ratio with aniline, hydrochloric acid (HCl) at 1:0.5 molar ratio with aniline and TiO_2 at 10 % weight content of aniline were added. The polymerization was performed at room temperature for another 120 min with continuous ultrasound; thus, polyester knit fabric with 1:0.1 ratio of polyaniline–TiO_2 was obtained and designated as $T_{0.1}$.

Similarly, the coated polyester knit fabrics of $T_{0.2}$, $T_{0.3}$, $T_{0.4}$, $T_{0.5}$, and T_0 without the incorporation of titanium dioxide were prepared, respectively. The schematic diagram of the preparation is shown in Fig. 1.

Characterization and measurement

Nicolet 5700 FTIR spectrometer (Thermo Nicolet Corporation, USA) with a wavenumber range of 500–4000 cm^{-1}

was used to analyze the fabric specimens. The morphological structures of coated polyester knit fabric were studied with scanning electron microscopy (SEM, JSM-5600LV). Thermal analysis was performed using an EXSTAR Model 6000 instrument. Abrasion test was carried out using fabric abrasion tester YG (B) 401T (Wenzhou Darong Textile Instrument Co., Ltd., China) according to ASTM D4966-10. Fabric bursting strength test was performed using DR028-300 (Wenzhou Darong Textile Instrument Co., Ltd., China) following ASTM D3787-2001.

Electrical sensitivity measurement

The surface electrical resistance of the resulting composite fabric was investigated according to the AATCC Test Method 76-2005.

The strain sensitivity of the prepared fabric was simulated by our setup apparatus, and the samples (6 cm × 2 cm) were located in YG-065 Electronic Fabric Strength Tester (Laizhou Electronic Instrument Co., Ltd., China) under a series of fixed vertical and horizontal elongations (10–60 %), respectively.

The electrical sensitivity coefficient of flexible fabric sensor was called nominal sensitivity coefficient, designated as "gauge factor" (GF). GF could be calculated from the electrical resistance rate ($\Delta R/R_0$) and strain rate ($\Delta L/L_0$) as follows:

$$\mathrm{GF} = \frac{\Delta R/R_0}{\varepsilon} = \frac{(R - R_0)/R_0}{\Delta L/L_0}, \tag{1}$$

where R is the surface electrical resistance under constant extension, R_0 the surface electrical resistance without extension, and $\varepsilon = \Delta L/L_0$ the fabric elongation under mechanical loading.

Furthermore, a parameter μ was introduced to indicate the relationship between static surface electrical resistance rate ($\Delta R/R_0$) and extension number (N), and the formula was as follows:

$$\mu = \frac{\Delta R}{R_0} = \frac{(R' - R_0)}{R_0} \times 100, \tag{2}$$

where ΔR indicates the difference between the surface electrical resistance R' after elongation (60 %) for specified durations and the initial surface electrical resistance R_0 without extension.

Water-repellent measurement

In this work, the water contact angle was used to characterize the water-repellent property of flexible fabric strain sensor. The wetting of the nanocomposite-coated fabric samples was studied by the sessile drop-contact angle measurement according to the method described in the reported literature [28, 31, 32].

Results and discussion

Characterization

The microstructure morphology of PANI and PANI/TiO_2 hybrid-coated PET knit fabric was studied by SEM, and the morphology of uncoated PET knit fabric was investigated for comparison. The typical results are shown in Fig. 2. Compared with uncoated PET knit fabric in Fig. 2a, the PANI granular film was uniformly deposited on PET knit fabric substrate under timely in situ polymerization conditions as in Fig. 2b. It can be seen from Fig. 2c that under the same polymerization condition, the PANI/TiO_2 hybrid film obtained is evenly distributed over the surface of the fabric. Moreover, it is reported that the morphology of polyaniline consists of a large number of honeycombed clews [33]. The honeycombed clews composed of interconnected network are favorable to increase the electrical conductivity. However, the existence of TiO_2 may hinder the carrier transport between different molecular chains of polyaniline which is prone to weaken the electrical conductivity of the hybrid-coated PET knit fabric. The dense hybrid film of PANI/TiO_2 is shown in Fig. 2c.

The FTIR spectra of hybrid-coated PET knit fabric and uncoated PET knit fabric are given in Fig. 3. The peak at 1575 cm^{-1} indicates the C=C stretching frequency of the quinoid ring of the PANI unit, whereas the peak at 1462 cm^{-1} indicates the C=C stretching of the benzenoid ring that shifts to 1485 cm^{-1} for both PANI-coated PET knit fabric (Fig. 3b) and PANI/TiO_2-coated PET knit fabric (Fig. 3c), respectively [34]. The bands at about 1298 cm^{-1} are attributed to C–N stretching mode for the benzenoid ring, and the band at 1109 cm^{-1} is assigned to a plane bending vibration of the C–H mode which is found during protonation; other peaks observed in the spectrum are due to the PET backbone [35, 36]. All these FTIR data show the formation of PANI for both composites. The peak at 615 cm^{-1} illustrates the Ti–O stretching frequency of the TiO_2 unit, thus confirming the formation of TiO_2 in PANI/TiO_2-coated PET knit fabric. It has been reported that when an oxidant is added to the reaction system, the polymerization starts initially on the surface of TiO_2 nanoparticles, and with the reaction proceeding the PANI is gradually deposited and forms a shell on the surface of TiO_2 nanoparticles. This may result from the adhesion of PANI to TiO_2 nanoparticles [37, 38].

The thermal properties of nanocomposites-coated PET knit fabric were analyzed using the thermogram shown in Fig. 4. As can be seen from the TG curves, there is weight loss due to moisture at the early stage and fiber and polyaniline degradation which occurs approximately between 400 and 500 °C. Furthermore, the weight gain of hybrid and TiO_2 content in hybrid-coated PET knit fabric has also

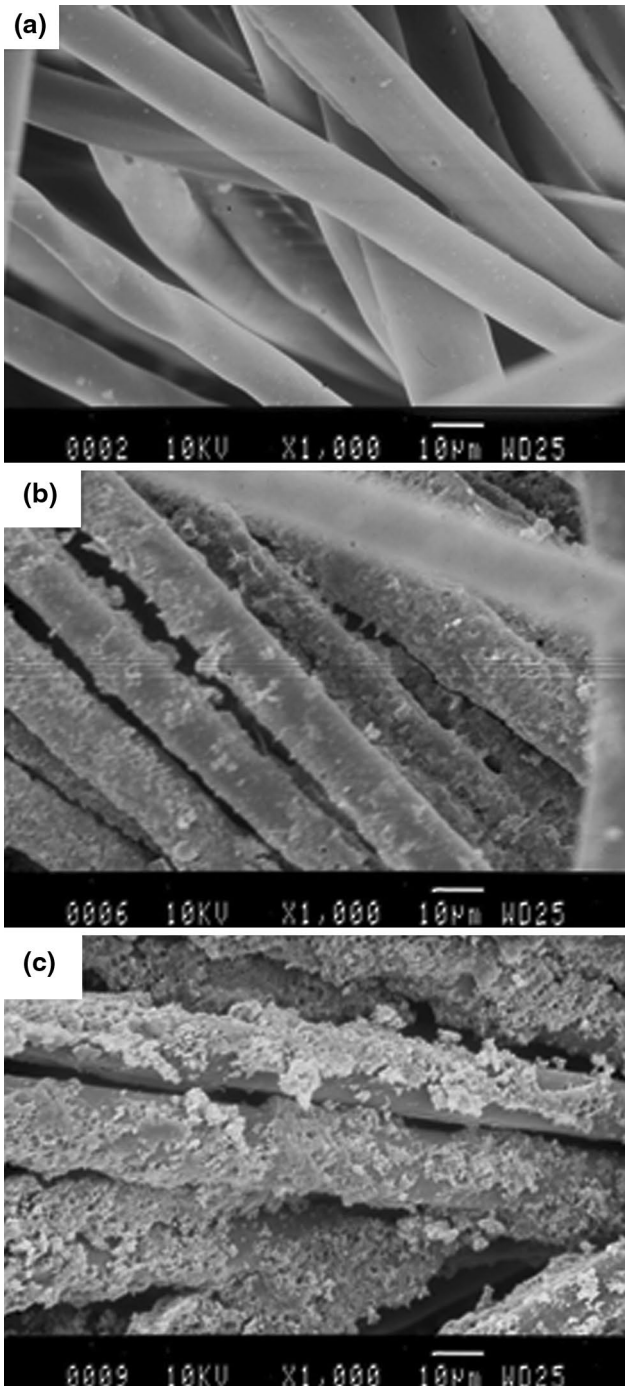

Fig. 2 SEM images of **a** uncoated PET knit fabric, **b** PANI-coated PET knit fabric and **c** PANI/TiO_2 hybrid-coated PET knit fabric

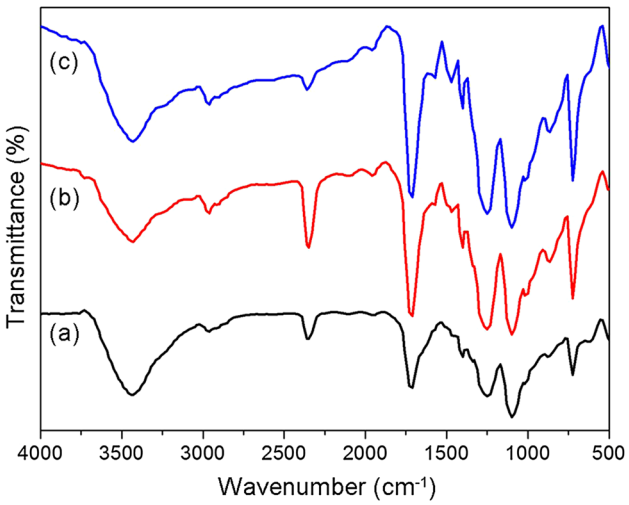

Fig. 3 FTIR spectra of *a* pure PET knit fabric, *b* PANI-coated PET knit fabric and *c* PANI/TiO_2-coated PET knit fabric of $T_{0.3}$

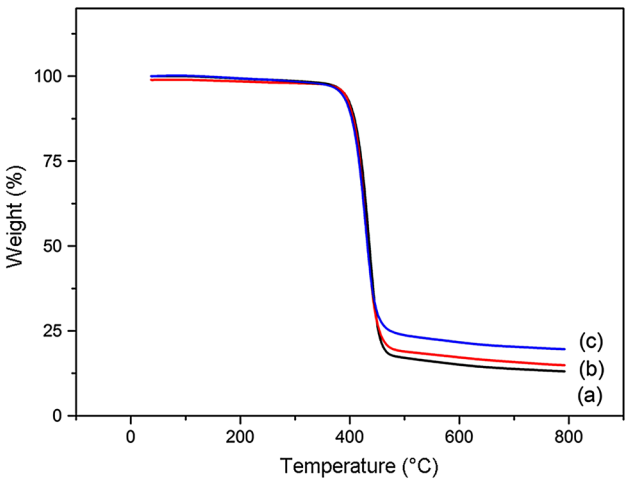

Fig. 4 Temperature-programmed TGA analysis curves of *a* control PET knit fabric, *b* pristine PANI-coated PET knit fabric and *c* PANI/TiO_2 hybrid-coated PET knit fabric of $T_{0.3}$

been revealed. The amount of hybrid present on the fabric calculated from the measurement of weight increasing experiment for T_0 was about 12.6 %, while it was 13.8 % weight increase for $T_{0.3}$. Moreover, the amount of TiO_2 content in $T_{0.3}$ PANI/TiO_2 nanocomposites-coated PET knit fabric was 4.65 % which can be calculated by the TG curve of Fig. 4a, c. This revealed that TiO_2 content in hybrid was approximately the same as that in the feed ratio in the polymerization process.

Electrical conductivity

The surface electrical resistance of PANI and PANI/TiO_2 hybrid-coated PET knit fabric, prepared under different polymerization conditions, was studied. Especially, the influence of TiO_2 concentration on the surface electrical resistance in the hydrothermal solution containing APS and hydrochloric acid (HCl) and the polymerization bath was investigated. The results are displayed in Fig. 5. The average electrical resistance of each sample is in the

range of 427–926 Ω cm. The electrical resistance of pristine PANI-coated PET knit fabric (T_0) was lower than that of PANI/TiO_2 hybrid-coated knit fabric. Furthermore, it can be inferred that the electrical resistance of the hybrid-coated knit fabric is in the order of $T_{0.1} > T_{0.2} > T_{0.3} < T_{0.4} < T_{0.5}$; this initial decrease in electrical resistance down to $T_{0.3}$ and subsequent increase are in agreement with previous reports. The decrease in surface electrical resistance by increasing the weight percent of TiO_2 in PANI for $T_{0.1}$ may be due to the particle blocking the conduction path by TiO_2 embedded in the PANI matrix [39]. Similarly, continuous increases in the weight percent of TiO_2 leads to a large number of polarons, where the inter-polaron coupling becomes progressively stronger even though there is disorderliness. This may lead to severe pinning of polarons and, therefore, restriction of the contribution at higher frequencies, hence reducing the electrical conductivity [40]. Moreover, the enhanced surface electrical conductivity of $T_{0.3}$ may be attributed to TiO_2 acting as suitable template for the formation of well-oriented polyaniline which is formed over the TiO_2 surface. However, the lower electrical conductivity of hybrid-coated fabrics with higher TiO_2 content may be due to the increased amount of TiO_2 which hinders the carrier transport trail between different molecular chains of polyaniline [41].

Electrical conductivity sensitivity

It can be concluded from Fig. 6 that the average gauge factor (GF) of vertical elongation may be arrived at 21.71 and 20.26, respectively, for T_0 and $T_{0.3}$, whereas the GF of horizontal elongation is just 2.25 and 2.06. The strain sensor of the electrical signal is obviously better vertically than horizontally, which may be in relation to the connection and slippage of knit loops. The yarn elongation is closely varied with fabric extension in the vertical direction, while the yarn elongation may be backward compared with fabric extension in the horizontal direction, considering the slippage and deformation of loops; thus the electrical sensitivity shows a lower value in the horizontal direction.

To evaluate the stability and strain sensitivity of surface electrical conductivity, recycled extension experiment was carried out under the condition of different numbers of stretching. As seen in the results in Fig. 7, the surface electrical resistance is increased with repeated number of elongations and changes slightly after 100 cycles of elongation. Also, the strain sensitivity of $T_{0.3}$ is better than that of T_0 in both the vertical and horizontal directions. Moreover, the excellent conductivity of PANI improves the charge carriers transfer rate in the composite; thus there is an increase in the separation efficiency of electron–hole pairs generated from TiO_2. Therefore,

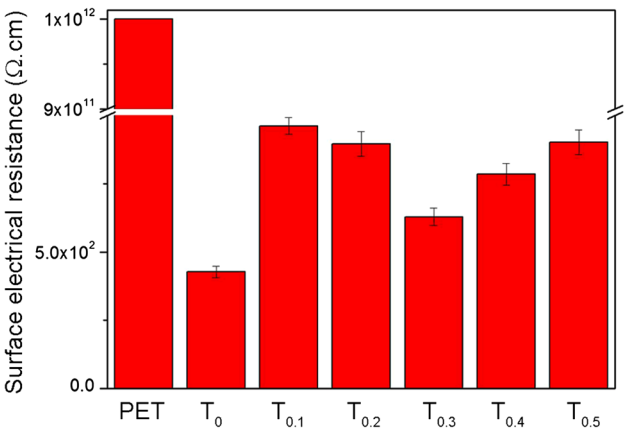

Fig. 5 The surface electrical resistance of pristine PET fabric (PET), pristine PANI-coated PET knit fabric (T_0) and hybrid-coated knit fabric with different TiO_2 contents ($T_{0.1} - T_{0.5}$)

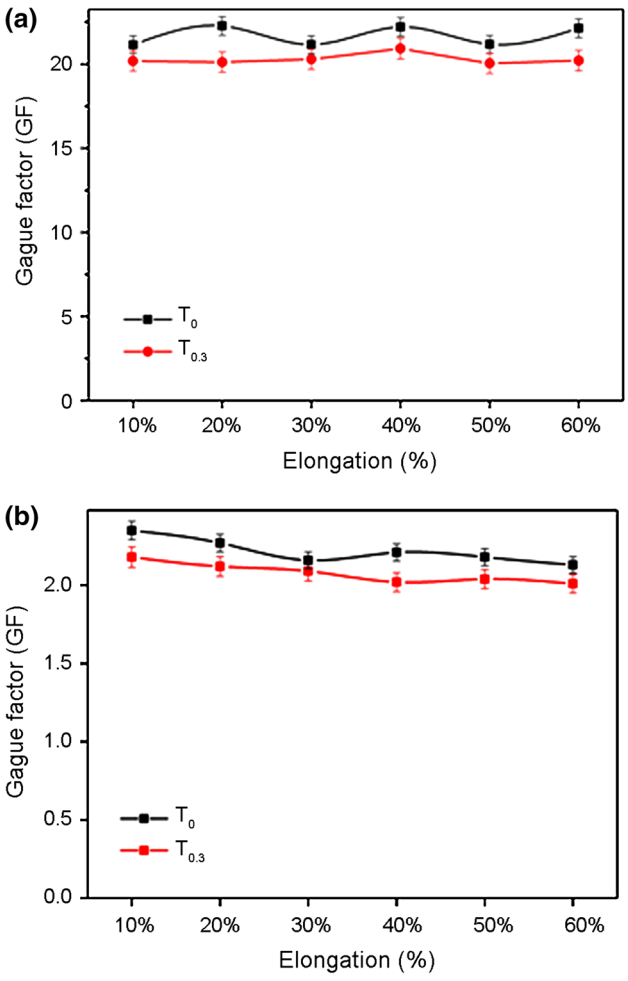

Fig. 6 Surface electrical conductivity sensitivity of PANI and PANI/TiO_2-coated PET knit fabric, **a** vertical elongation and **b** horizontal elongation

the lifetime of charge carrier generated from the photocatalyst is prolonged, and the stability of electrical strain sensitivity is also enhanced [42, 43].

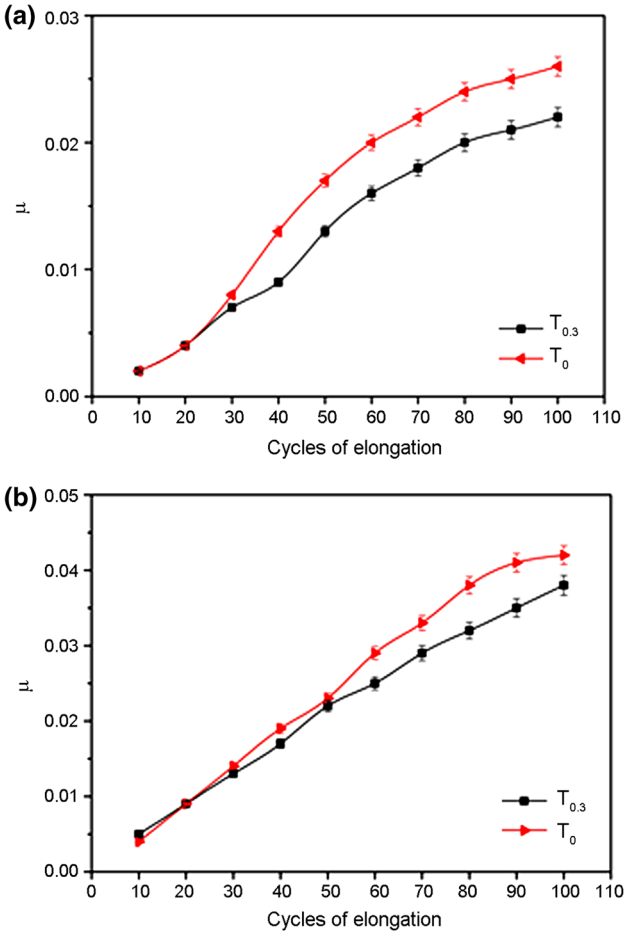

Fig. 7 Stability of electrical conductivity sensitivity (μ) of PANI and PANI/TiO_2-coated PET knit fabric, **a** vertical elongation and **b** horizontal elongation

Water-repellent properties

Flexible fabric strain sensor treated with polyaniline/TiO_2 nanocomposites could obtain excellent water-repellent properties as seen in Fig. 8. It is also obvious that the dark green polyaniline is changed to lighter color due to the presence of TiO_2 nanoparticles as shown in Fig. 8b, c. The corresponding water contact angle shown in Table 1 could reach a desirable level (127.5° ± 1.7°), as the fabric was modified and it could also preserve reasonable water-repellent properties (121.8° ± 2.6°) even after 100 cycles of elongation. As mentioned in the reported literature [44–46], the presence of TiO_2 nanoparticles and surface roughness ensure excellent water-repellent efficiency. With the water contact angles higher than 120°, measured for PANI/TiO_2 nanocomposites deposited on fabric surface even after 100 cycles of elongation, the flexible fabric strain sensor can be considered as a fabric with excellent water-repellent properties.

Mechanical properties

The mechanical properties of polyester knit fabric before and after polymerization are shown in Table 2. Surface abrasion test was performed to investigate the service durability and interface bonding strength of hybrids on fabric substrate. Furthermore, bursting strength measurement was carried out to evaluate the mechanical strength. Pristine polyaniline-coated polyester knit fabric (T_0) could withstand just for 100 abrasions and then torn off. This proves that pristine polyaniline-coated fabric becomes physically weak due to the damage made by acid-based medium in the polymerization solution. However, the abrasion resistance of the prepared fabric increases with the increase of TiO_2, and the hybrid-coated fabrics ($T_{0.3}$, $T_{0.4}$ and $T_{0.5}$) are strong enough to withstand more than 160 cycles. This demonstrates that there is only little loss in service durability for

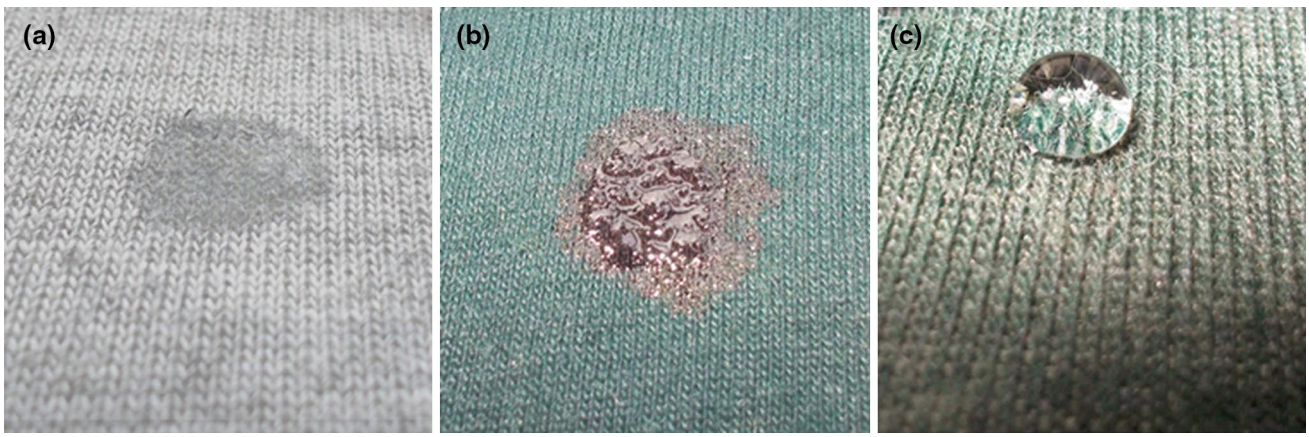

Fig. 8 Distilled water droplet on the flexible fabric strain sensor, **a** control fabric, **b** pristine polyaniline-coated fabric and **c** polyaniline/TiO_2-coated fabric ($T_{0.3}$)

Table 1 Water contact angles during the cycles of elongation

Cycles of elongation	Water contact angle (°)		
	Control fabric	Pristine PANI-coated fabric	PANI–TiO_2-coated fabric ($T_{0.3}$)
0	82.1 ± 2.1	83.5 ± 2.2	127.5 ± 1.8
10	81.6 ± 2.0	83.1 ± 2.7	128.1 ± 2.8
20	81.8 ± 2.2	81.6 ± 2.8	127.2 ± 2.6
30	81.5 ± 2.0	82.6 ± 2.4	126.4 ± 2.8
40	80.2 ± 2.8	82.1 ± 1.8	125.2 ± 2.1
50	81.0 ± 2.4	81.5 ± 2.9	125.5 ± 2.0
60	80.5 ± 2.0	82.0 ± 3.1	123.3 ± 2.4
70	79.8 ± 2.3	81.9 ± 2.7	123.9 ± 2.7
80	79.6 ± 1.9	81.8 ± 2.3	122.1 ± 1.9
90	80.4 ± 2.5	81.6 ± 2.8	121.5 ± 2.2
100	79.5 ± 2.6	81.2 ± 2.1	121.8 ± 2.6

Table 2 Mechanical strength before and after polymerization

Sample	Number of abrasion cycles withstand	Bursting strength/*N*
Untreated fabric	226	586
T_0	98	352
$T_{0.1}$	105	396
$T_{0.2}$	128	456
$T_{0.3}$	167	461
$T_{0.4}$	171	450
$T_{0.5}$	163	462

hybrid-coated fabric when compared to uncoated polyester knit fabric which withstands 226 cycles. The results of bursting strength testing are also shown in Table 2; in general, the polymerization process decreases the strength of the prepared flexible fabric strain sensor. Similar to the abrasion resistance, bursting strength improved with the incorporation of TiO_2. The bursting strength of hybrid-coated fabrics ($T_{0.2}$, $T_{0.3}$, $T_{0.4}$ and $T_{0.5}$) is higher than 450 N, which is just slightly decreased compared with untreated polyester knit fabric (bursting strength of 586 N). This suggests that the TiO_2 part acts as a binding material to improve the physical properties of the prepared fabric, which is in accordance with the literature [27, 41]. Thus, the prepared flexible fabric strain sensor containing polyaniline/TiO_2 hybrid coating has better service durability and strength than pristine polyaniline-coated fabric.

Conclusion

In conclusion, flexible fabric strain sensor based on PANI/TiO_2 nanocomposites-coated knit polyester fabric could be successfully fabricated via an in situ polymerization method. The prepared flexible fabric strain sensor performed better sensitivity than pristine PANI-based flexible fabric strain sensor, although the surface electrical conductivity did decrease slightly. According to the experiments, PANI/TiO_2 nanocomposites-coated flexible fabric strain sensor exhibited excellent water-repellent efficiency and good durability during the cycles of elongation. The PANI/TiO_2 nanocomposite-coated polyester knit fabrics as promising flexible fabric strain sensors are expected to find wide applications in sensing garment, wearable hardware and intelligent materials for the preparation of smart wearable devices.

Acknowledgments This work is supported by the Natural Science Foundation of China (Nos. 51273097 and 51306095), China Postdoctoral Science Foundation via Grant No. 2014M561887 and Taishan Scholars Construction Engineering of Shandong Province, program for scientific research innovation team in colleges and universities of Shandong Province, Collaborative Innovation Center for Marine Biomass Fibers, Materials and Textiles of Shandong Province.

References

1. Mondal S (2008) Phase change materials for smart textiles—an overview. Appl Therm Eng 28:1536–1550
2. Farringdon J, Moore AJ, Tilbury N, Church J, Biemond PD (1999) Wearable sensor badge and sensor jacket for context awareness. Wearable computers, 1999 digest of papers. The 3rd international symposium on IEEE 107–113
3. Rossi D, Lorussi F, Mazzoldi A, Orsini P, Scilingo E (2003) Sensors and sensing in biology and engineering. Springer, Wien
4. Scilingo EP, Lorussi F, Mazzoldi A, De Rossi D (2003) Strain-sensing fabrics for wearable kinaesthetic-like systems. Sens J 3:460–467
5. Kuo H, Hsui TF, Tuo Y, Yuan C (2012) Microwave adsorption of core–shell structured $Sr(MnTi)_xFe_{12-2x}O_{19}$/PANI composites. J Mater Sci 47:2264–2270
6. Dhingra M, Shrivastava S, Senthil Kumar P, Annapoorni S (2013) Polyaniline mediated enhancement in band gap emission of zinc oxide. Compos B 45:1515–1520

7. Ansari R, Alizadeh N, Shademan SM (2013) Application of silica gel/polyaniline composite for adsorption of ascorbic acid from aqueous solutions. Iran Polym J 22:739–748
8. Zare EN, Lakouraj MM (2014) Biodegradable polyaniline/dextrin conductive nanocomposites: synthesis, characterization, and study of antioxidant activity and sorption of heavy metal ions. Iran Polym J 23:257–266
9. Yan H, Kou K (2014) Enhanced thermoelectric properties in polyaniline composites with polyaniline-coated carbon nanotubes. J Mater Sci 49:1222–1228
10. Wang G, Xing W, Zhuo S (2012) The production of polyaniline/graphene hybrids for use as a counter electrode in dye-sensitized solar cells. Electrochim Acta 66:151–157
11. Konwer S, Guha AK, Dolui SK (2013) Graphene oxide-filled conducting polyaniline composites as methanol-sensing materials. J Mater Sci 48:1729–1739
12. Li L, Song H, Zhang Q, Yao J, Chen X (2009) Effect of compounding process on the structure and electrochemical properties of ordered mesoporous carbon/polyaniline composites as electrodes for supercapacitors. J Power Sources 187:268–274
13. Patil S, Chougule M, Sen S, Patil V (2012) Measurements on room temperature gas sensing properties of CSA doped polyaniline–ZnO nanocomposites. Measurement 45:243–249
14. Zhao YP, Cai ZS, Zhou ZY, Fu XL (2011) Fabrication of conductive network formed by polyaniline–ZnO composite on fabric surfaces. Thin Solid Films 519:5887–5891
15. Yilmaz H, Zengin H, Unal HI (2012) Synthesis and electrorheological properties of polyaniline/silicon dioxide composites. J Mater Sci 47:5276–5286
16. Shambharkar BH, Umare SS (2011) Synthesis and characterization of polyaniline/NiO nanocomposite. J Appl Polym Sci 122:1905–1912
17. Saini P, Choudhary V, Vijayan N, Kotnala RK (2012) Improved electromagnetic interference shielding response of poly(aniline)-coated fabrics containing dielectric and magnetic nanoparticles. J Phys Chem C 116:13403–13412
18. Kachoei Z, Khoee S, Sanjani NS (2015) Well-designed sandwich-like structured graphene/emeraldine salts prepared by inverse microemulsion polymerization with particle-on-sheet and sheet-on-sheet morphologies. Iran Polym J 24:203–217
19. Ashraf R, Kausar A, Siddiq M (2014) High-performance polymer/nanodiamond composites: synthesis and properties. Iran Polym J 23:531–545
20. Ferrero F, Periolatto M (2013) Application of fluorinated compounds to cotton fabrics via sol–gel. Appl Surf Sci 275:201–207
21. Chen X, Mao SS (2007) Titanium dioxide nanomaterials: synthesis, properties, modifications, and applications. Chem Rev 107:2891–2959
22. Wu M, Zhang F, Yu J, Zhou H, Zhang D, Hu C, Huang J (2014) Fabrication and evaluation of light-curing nanocomposite resins filled with surface-modified TiO_2 nanoparticles for dental application. Iran Polym J 23:513–524
23. Li GJ, Fan SR, Wang K, Ren XL, Mu XW (2010) Modification of TiO_2 with titanate coupling agent and its impact on the crystallization behaviour of polybutylene terephthalate. Iran Polym J 19:115–121
24. Bowman D, Mattes BR (2005) Conductive fibre prepared from ultra-high molecular weight polyaniline for smart fabric and interactive textile applications. Synth Met 154:29–32
25. Kim BS, Lee KT, Huh PH, Lee DH, Jo NJ, Lee JO (2009) In situ template polymerization of aniline on the surface of negatively charged TiO_2 nanoparticles. Synth Met 159:1369–1372
26. Xiong S, Wang Q, Xia H (2004) Template synthesis of polyaniline/TiO_2 bilayer microtubes. Synth Met 146:37–42
27. Savitha KU, Prabu HG (2013) Polyaniline–TiO_2 hybrid-coated cotton fabric for durable electrical conductivity. J Appl Polym Sci 127:3147–3151
28. Tang X, Tian M, Qu L, Zhu S, Guo X, Han G, Sun K, Hu X, Wang Y, Xu X (2014) A facile fabrication of multifunctional knit polyester fabric based on chitosan and polyaniline polymer nanocomposite. Appl Surf Sci 317:505–510
29. Arenas M, Sanchez G, Martinez-Alvarez O, Castaño V (2014) Electrical and morphological properties of polyaniline–polyvinyl alcohol in situ nanocomposites. Compos B 56:857–861
30. Hong GB, Su TL (2012) Statistical analysis of experimental parameters in characterization of ultraviolet-resistant polyester fiber using a TOPSIS-Taguchi method. Iran Polym J 21:877–885
31. Ivanova NA, Philipchenko AB (2012) Superhydrophobic chitosan-based coatings for textile processing. Appl Surf Sci 263:783–787
32. Emelyanenko AM, Ermolenko NV, Boinovich LB (2004) Contact angle and wetting hysteresis measurements by digital image processing of the drop on a vertical filament. Colloids Surf A Physicochem Eng Asp 239:25–31
33. Chao D, Chen J, Lu X, Chen L, Zhang W, Wei Y (2005) SEM study of the morphology of high molecular weight polyaniline. Synth Met 150:47–51
34. Sathiyanarayanan S, Azim SS, Venkatachari G (2007) A new corrosion protection coating with polyaniline–TiO_2 composite for steel. Electrochim Acta 52:2068–2074
35. Girija T, Sangaranarayanan M (2006) Polyaniline-based nickel electrodes for electrochemical supercapacitors—influence of Triton X-100. J Power Sources 159:1519–1526
36. Ghosh D, Giri S, Kalra S, Das CK (2012) Synthesis and characterisations of TiO_2 coated multiwalled carbon nanotubes/graphene/polyaniline nanocomposite for supercapacitor applications. Open J Appl Sci 2:70–77
37. Xia H, Wang Q, Qiu G (2003) Polymer-encapsulated carbon nanotubes prepared through ultrasonically initiated in situ emulsion polymerization. Chem Mater 15:3879–3886
38. Min S, Wang F, Han Y (2007) An investigation on synthesis and photocatalytic activity of polyaniline sensitized nanocrystalline TiO_2 composites. J Mater Sci 42:9966–9972
39. Manjunath S, Anilkumar KR, Revanasiddappa M, Ambika Prasad M (2008) Frequency-dependent conductivity and dielectric permittivity of polyaniline/TiO_2 composites. Ferroelectr Lett 35:36–46
40. Javadi H, Cromack K, MacDiarmid A, Epstein A (1989) Microwave transport in the emeraldine form of polyaniline. Phys Rev B 39:3579
41. Unnikrishnan SK, Vinayasree S, Halliah GP, Anantharaman MR (2013) Flexible electromagnetic interference shields in S band region from textile materials. J Ind Text 43:215–230
42. Lin Y, Li D, Hu J, Xiao G, Wang J, Li W, Fu X (2012) Highly efficient photocatalytic degradation of organic pollutants by PANI–modified TiO_2 composite. J Phys Chem C 116:5764–5772
43. Li Y, Yu Y, Wu L, Zhi J (2013) Processable polyaniline/titania nanocomposites with good photocatalyic and conductivity properties prepared via peroxo-titanium complex catalyzed emulsion polymerization approach. Appl Surf Sci 273:135–143
44. Qu M, Zhao G, Cao X, Zhang J (2008) Biomimetic fabrication of lotus-leaf-like structured polyaniline film with stable superhydrophobic and conductive properties. Langmuir 24:4185–4189
45. Ganesh VA, Dinachali SS, Nair AS, Ramakrishna S (2013) Robust superamphiphobic film from electrospun TiO_2 nanostructures. ACS Appl Mater Interfaces 5:1527–1532
46. Lai Y, Lin C, Huang J, Zhuang H, Sun L, Nguyen T (2008) Markedly controllable adhesion of superhydrophobic spongelike nanostructure TiO_2 films. Langmuir 24:3867–3873